The EMBO Journal (2004) 23, 169–179 | © 2004 European Molecular Biology Organization | All Rights Reserved 0261-4189/04
www.embojournal.org

THE EMBO JOURNAL

Cytoprotection by pre-emptive conditional phosphorylation of translation initiation factor 2

Phoebe D Lu[1], Céline Jousse[1], Stefan J Marciniak[1], Yuhong Zhang[1], Isabel Novoa[1], Donalyn Scheuner[2], Randal J Kaufman[2], David Ron[1,*] and Heather P Harding[3]

[1]Skirball Institute, New York University School of Medicine, New York, NY, USA, [2]Howard Hughes Medical Institute and the Department of Biochemistry, University of Michigan School of Medicine, Ann Arbor, MI, USA and [3]Department of Pharmacology, New York University School of Medicine, New York, NY, USA

Transient phosphorylation of the α-subunit of translation initiation factor 2 (eIF2α) represses translation and activates select gene expression under diverse stressful conditions. Defects in the eIF2α phosphorylation-dependent integrated stress response impair resistance to accumulation of malfolded proteins in the endoplasmic reticulum (ER stress), to oxidative stress and to nutrient deprivations. To study the hypothesized protective role of eIF2α phosphorylation in isolation of parallel stress signaling pathways, we fused the kinase domain of pancreatic endoplasmic reticulum kinase (PERK), an ER stress-inducible eIF2α kinase that is normally activated by dimerization, to a protein module that binds a small dimerizer molecule. The activity of this artificial eIF2α kinase, Fv2E-PERK, is subordinate to the dimerizer and is uncoupled from upstream stress signaling. Fv2E-PERK activation enhanced the expression of numerous stress-induced genes and protected cells from the lethal effects of oxidants, peroxynitrite donors and ER stress. Our findings indicate that eIF2α phosphorylation can initiate signaling in a cytoprotective gene expression pathway independently of other parallel stress-induced signals and that activation of this pathway can single-handedly promote a stress-resistant preconditioned state.

The EMBO Journal (2004) **23,** 169–179. doi:10.1038/sj.emboj.7600030; Published online 8 January 2004
Subject Categories: proteins; cellular metabolism
Keywords: preconditioning; protein kinases; reactive oxygen species; signal transduction; translation

Abbreviations: ISR, integrated stress response; eIF2, eukaryotic translation initiation factor-2; PERK, pancreatic endoplasmic reticulum kinase; ATF4, activating transcription factor 4; GADD34, growth arrest and DNA damage gene 34; CHOP, C/EBP homologous proteins; DCF, dichlorofluorescein; β-ME, β-mercaptoethanol

*Corresponding authors. Skirball Institute, New York University School of Medicine, Third Floor, Lab 10, 540 First Avenue, New York, NY 10016, USA. Tel.: +1 212 263 7786; Fax: +1 212 263 8951;
E-mail: ron@saturn.med.nyu.edu
E-mail: harding@saturn.med.nyu.edu

Received: 23 June 2003; accepted: 27 October 2003; Published online: 8 January 2004

Introduction

Four protein kinases are known to couple the otherwise unrelated stresses of protein malfolding in the endoplasmic reticulum (ER) (Ron and Harding, 2000), amino acid deprivation (Hinnebusch, 2000), viral infection (Kaufman, 2000) and heme deficiency (Chen, 2000) to the phosphorylation of translation initiation factor 2 on serine 51 of its alpha subunit (eIF2α). This results in inhibition of the guanine nucleotide exchange factor of the eIF2 complex, repressing mRNA translation and protein synthesis (Hinnebusch, 2000; Dever, 2002). At the same time the translation of activating transcription factor 4 (*ATF4*) mRNA is specifically increased (Harding *et al*, 2000a). We have recently discovered that ATF4 plays an important role in activating genes that promote the linked processes of import and metabolism of thiol-containing amino acids and resistance to oxidative stress. Because it integrates signaling in diverse stressful conditions, we refer to this eIF2α phosphorylation-dependent, stress-inducible pathway as an integrated stress response (ISR) (Harding *et al*, 2003).

Various lines of evidence point to a possible role for eIF2α phosphorylation in promoting resistance to cellular stresses. Mutations in the upstream eIF2α kinases pancreatic endoplasmic reticulum kinase (PERK) and GCN2 compromise resistance to ER stress and nutritional deprivation, respectively (Harding *et al*, 2000b; Harding *et al*, 2001; Zhang *et al*, 2002a, b), and replacing serine 51 in eIF2α with an alanine, a mutation that precludes phosphorylation by the stress-activated kinases, also markedly sensitizes cells to stress (Scheuner *et al*, 2001). In other pathophysiological contexts, it has been noted that cerebral ischemia results in profound but transient eIF2α phosphorylation and activates some of the target genes of the ISR (DeGracia *et al*, 2002). The latter process has been linked to the activity of the eIF2α kinase PERK (Kumar *et al*, 2001), which promotes resistance to the stress of malfolded proteins in the ER. Hibernation in mammals, which is one of the most stress-resistant states of the central nervous system, is associated with very high levels of eIF2α phosphorylation (Frerichs and Hallenbeck, 1998; Frerichs *et al*, 1998). Lastly, stable genetic manipulations that constitutively reduced the activity of the eIF2 complex (and thereby phenocopy the effects of eIF2α phosphorylation) induce a state of resistance to oxidative glutamate toxicity in an immortalized mouse hippocampal cell line (Tan *et al*, 2001).

It has long been known that low levels of stress that activate downstream signaling pathways without causing severe cell injury can protect against subsequent exposure to more severe stress. This phenomenon is referred to as preconditioning and has a significant heterologous component such that the preconditioning stimulus and the subsequent stress may be very different in nature. Pathways, such as the ISR, that couple diverse stressful conditions to a common downstream event (eIF2α phosphorylation) are

candidates for having a role in heterologous preconditioning. This idea is further supported by the aforementioned study of Schubert and colleagues, which demonstrated a protective role for stable genetic manipulations that reduce the activity of the eIF2 complex (Tan *et al*, 2001). However, as the conditions known to activate eIF2α kinases are invariably stressful, it has not been possible to segregate the contribution of other parallel signaling pathways that operate alongside eIF2α phosphorylation from the contribution of eIF2α phosphorylation to heterologous preconditioning. Nor is it known which, if any, of the components of the ISR can be activated purely by eIF2α phosphorylation. These questions are relevant both to understanding the details of signaling pathways operative during cell stress and to the practical issue of identifying components of these pathways that might serve as useful targets for interventions to promote pharmacological preconditioning.

To determine if signaling by phosphorylated eIF2α and activation of the ISR may be harnessed to promote preconditioning, we have created a genetic system for inducing rapid reversible phosphorylation of eIF2α independently of cell stress and examined its impact on the susceptibility of cultured cells to diverse stressful conditions.

Results

Stress associated with eIF2α phosphorylation protects HT22 cells against oxidative glutamate toxicity

Extracellular glutamate depletes intracellular cysteine and glutathione, leading to oxidative glutamate toxicity (Murphy *et al*, 1989), a process believed to play a role in neuronal cell death mediated by extracellular glutamate (Schubert and Piasecki, 2001). HT22 cells are an immortal mouse hippocampal cell line that is resistant to glutamatergic excitotoxicity but susceptible to oxidative glutamate toxicity and represents a useful model system for studying cellular responses to oxidative stress (Morimoto and Koshland, 1990; Maher and Davis, 1996; Tan *et al*, 2001). To test the hypothesis that eIF2α phosphorylation and activation of the ISR promotes resistance to oxidative glutamate toxicity, we first measured the ability of manipulations known to promote eIF2α phosphorylation to protect HT22 cells from the lethal effects of glutamate. Pretreatment of HT22 cells with tunicamycin or thapsigargin, ER stress-inducing agents that cause eIF2α phosphorylation and activate the ISR (Harding *et al*, 2003), was protective against subsequent challenge with glutamate (Figure 1A).

The stress paradigm used, 1 h treatment with the ER stress-inducing drug followed by 5 h recovery before exposure to glutamate, was sufficient to induce both eIF2α phosphorylation and subsequent expression of the ISR targets ATF4, GADD34 and CHOP (Figure 1B). The survival benefit was dose-dependent and the protective effect of the different stressors correlated with their ability to promote eIF2α phosphorylation (data not shown). The brief interval between the preconditioning ER stress and application of glutamate favors a true survival advantage afforded by the preceding stress and discounts selection for stress-resistant cells and their proliferation at the expense of a susceptible sub-population as the basis for the increased survival of the pretreated cells. We conclude that stressful manipulations that increase the

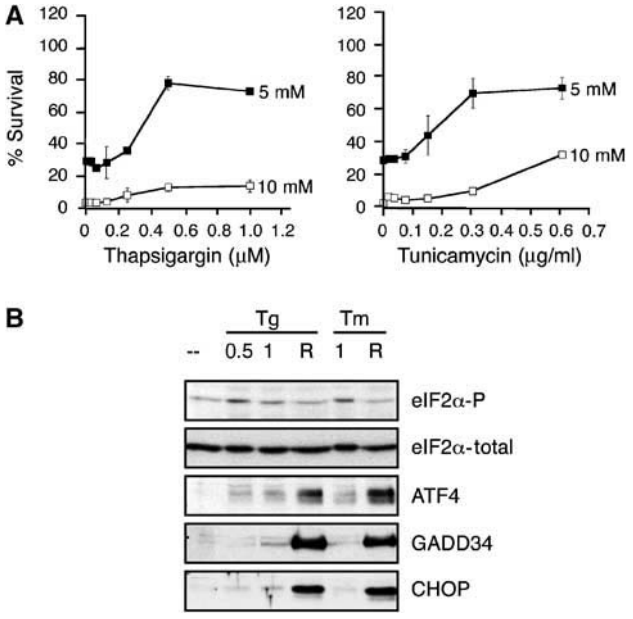

Figure 1 Stresses that promote eIF2α phosphorylation protect HT22 cells from glutamate-induced cell death. **(A)** Survival of HT22 cells pretreated for 1 h with thapsigargin or tunicamycin followed by 5 h of recovery and subsequent challenge with 5 mM glutamate (closed squares) or 10 mM glutamate (open squares) for 24 h. Survival is expressed as a percentage of MTT reduced by glutamate-treated cells in each pretreatment group compared with MTT reduction by cells subjected to the same pretreatment but not exposed to glutamate. Values shown are the mean and SEM from a representative experiment performed in triplicate and reproduced twice. **(B)** Immunoblots of cytoplasmic extracts incubated with antisera specific for phosphorylated eIF2α (eIF2α-P), total eIF2α and GADD34 and of nuclear extracts incubated with antisera to ATF4 and CHOP from untreated HT22 cells, or cells treated with thapsigargin (Tg, 0.5 μM) or tunicamycin (Tm, 0.3 μg/ml) for 0.5 or 1 h and after 5 h of recovery (R).

level of phosphorylated eIF2α promote resistance to glutamate toxicity in HT22 cells.

To further examine the correlation between eIF2α phosphorylation and resistance to glutamate, we measured the impact of blocking eIF2α phosphorylation in HT22 cells. To this end, we overexpressed an activated form of GADD34, the regulatory subunit of an eIF2α-specific holophosphatase complex, in HT22 cells (Novoa *et al*, 2001). As predicted, HT22 cells that stably overexpressed an active fragment of GADD34 had no detectable phosphorylated eIF2α under basal conditions or when stressed (Figure 2A). Inhibition of eIF2α phosphorylation markedly compromised cell survival in regular media. However, the defect was rescued by adding the reducing compound β-mercaptoethanol (βME) to the media (Figure 2B and C). These observations indicate a role for eIF2α phosphorylation in the basal resistance of HT22 cells to oxidative stress and are consistent with the phenotype of mouse embryonic fibroblasts (MEFs) with a compromised ISR (Harding *et al*, 2003).

Cells cultured in media containing anti-oxidants such as βME are resistant to cell death induced by 5 mM glutamate (Miyamoto *et al*, 1989; Davis and Maher, 1994) (and data not shown). However, we found that susceptibility to glutamate toxicity could be restored if cells previously growing in the media containing βME were switched to media lacking βME during the exposure to glutamate. About 20% of parental

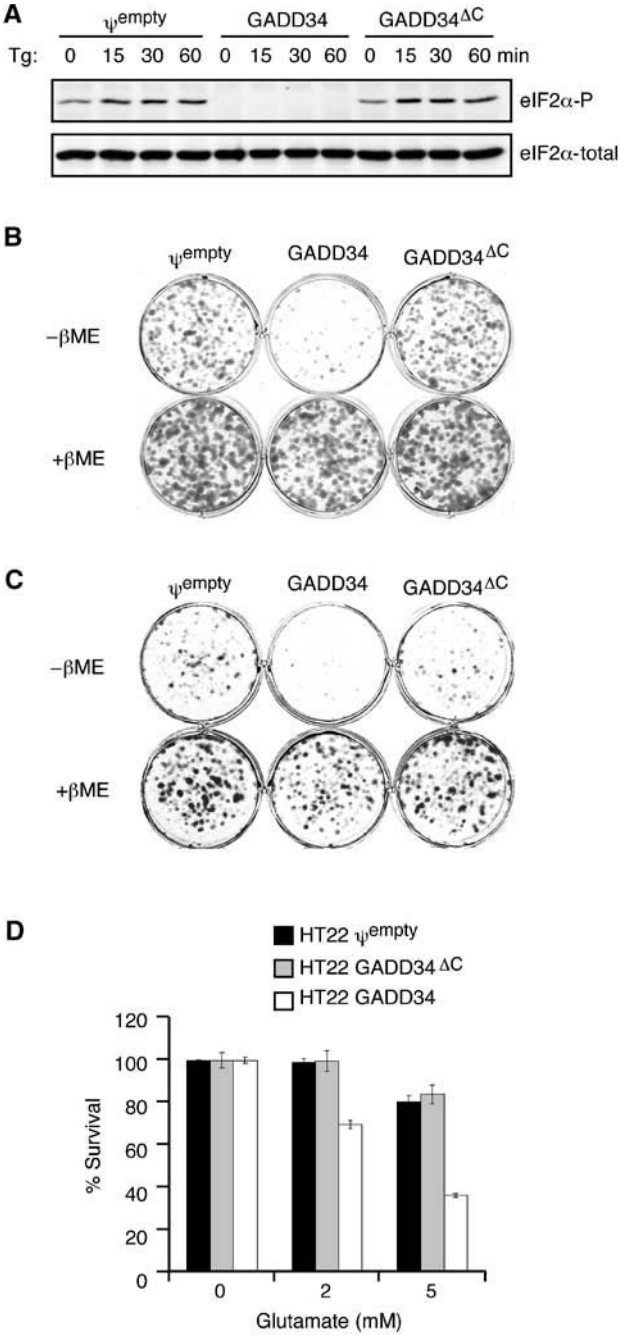

Figure 2 Impaired eIF2α phosphorylation sensitizes HT22 cells to oxidative glutamate toxicity. (**A**) Immunoblot of phosphorylated eIF2α (eIF2α-P) and total eIF2α from ψ^{empty}, GADD34 or GADD34$^{\Delta C}$ cells treated with 400 nM thapsigargin (Tg) for the indicated time. (**B**) Photomicrograph of crystal-violet-stained HT22 cells transduced with retroviruses expressing an activated form of an eIF2α phosphatase (GADD34), an inactive mutant (GADD34$^{\Delta C}$) or the empty vector (ψ^{empty}). Following transduction, cells were plated at clonal density and cultured in regular media or media supplemented with the reducing compound βME for 6 days prior to staining. (**C**) Photomicrograph of crystal-violet-stained HT22 cells selected for stable expression of GADD34, ψ^{empty} or GADD34$^{\Delta C}$ and plated at clonal density regular in media or media containing βME. (**D**) Survival of HT22 GADD34, ψ^{empty} or GADD34$^{\Delta C}$ cells following 24 h of exposure to glutamate in media lacking βME. 100% survival is defined as the MTT reduction by cells of each line that had not been exposed to glutamate. The graph shown represents a typical experiment performed in duplicate and reproduced twice.

HT22 cells, previously cultured in βME, were dead after 24 h exposure to 5 mM glutamate in media lacking βME (Figure 2D). This compared with ~65% death following a similar exposure in cells that had not been cultured previously in βME -containing media (Figures 1A and 4C). In this paradigm of switch from βME (+) to βME (−), GADD34-overexpressing HT22 cells were hypersensitive to cell death induced by glutamate treatment. Only 70% of such cells survived 24 h exposure in 2 mM glutamate, as compared to 100% survival of the inactive GADD34$^{\Delta C}$-overexpressing control cells or cells transduced with empty vector. Following exposure to 5 mM glutamate, there was 36% survival of GADD34-overexpressing HT22 cells compared with approximately 80% survival in the control cell lines (Figure 2D). Withdrawal of the βME for the period of time used for glutamate exposure did not compromise survival of the GADD34-expressing HT22 or the control cells (data not shown). This experiment indicates that blocking eIF2α phosphorylation sensitizes HT22 cells to oxidative glutamate toxicity.

A ligand-activated eIF2α kinase that promotes conditional translational inhibition and downstream target gene expression

The experiments described above establish a correlation between eIF2α phosphorylation and resistance to oxidative glutamate toxicity. However, many signaling pathways are activated in stressed cells and it was therefore impossible to attribute the protective effect of the preconditioning preceding stress specifically to eIF2α phosphorylation and activation of the ISR. To uncouple eIF2α phosphorylation from stress, we took advantage of the fact that activation of PERK is initiated by oligomerization, which leads to *trans*-autophosphorylation and increased ability to phosphorylate its substrate, eIF2α. Normally, this oligomerization event is driven by the stress-sensing ER lumenal domain of PERK; however PERK activation can be subordinated to any heterologous oligomerization domain (Bertolotti *et al*, 2000; Liu *et al*, 2000). Therefore, we fused the eIF2α kinase effector domain of PERK to a polypeptide containing two modified FK506 binding domains (Fv2E) and expressed the fusion protein, Fv2E-PERK, as a soluble cytoplasmic protein in HT22 cells (Figure 3A). The modified FKBP domain (Fv2E) is a high-affinity receptor for a cell-permeant synthetic small organic molecule, AP20187, that can be engaged simultaneously by two modified Fv2E domains (Spencer *et al*, 1993). The bivalent ligand thereby serves as a dimerizer/oligomerizer, and when added to cells can induce clustering of Fv2E-containing fusion proteins.

Because it lacks an ER lumenal domain, Fv2E-PERK does not respond to ER stress but allows for drug-induced activation of the eIF2α kinase domain of PERK without subjecting the cells to ER stress. Addition of AP20187 to Fv2E-PERK-expressing HT22 cells resulted in rapid activation of the kinase as reflected in a shift to a slower mobility *trans*-autophosphorylated form (Figure 3B). Fv2E-PERK remains phosphorylated for the duration of exposure of cells to AP20187. Furthermore, phosphorylation of endogenous eIF2α approaches saturation within 15 min and expression of the ISR target genes, GADD34 and CHOP, was observed within 2 h of drug treatment. AP20187 has no impact on eIF2α phosphorylation or target gene expression in parental

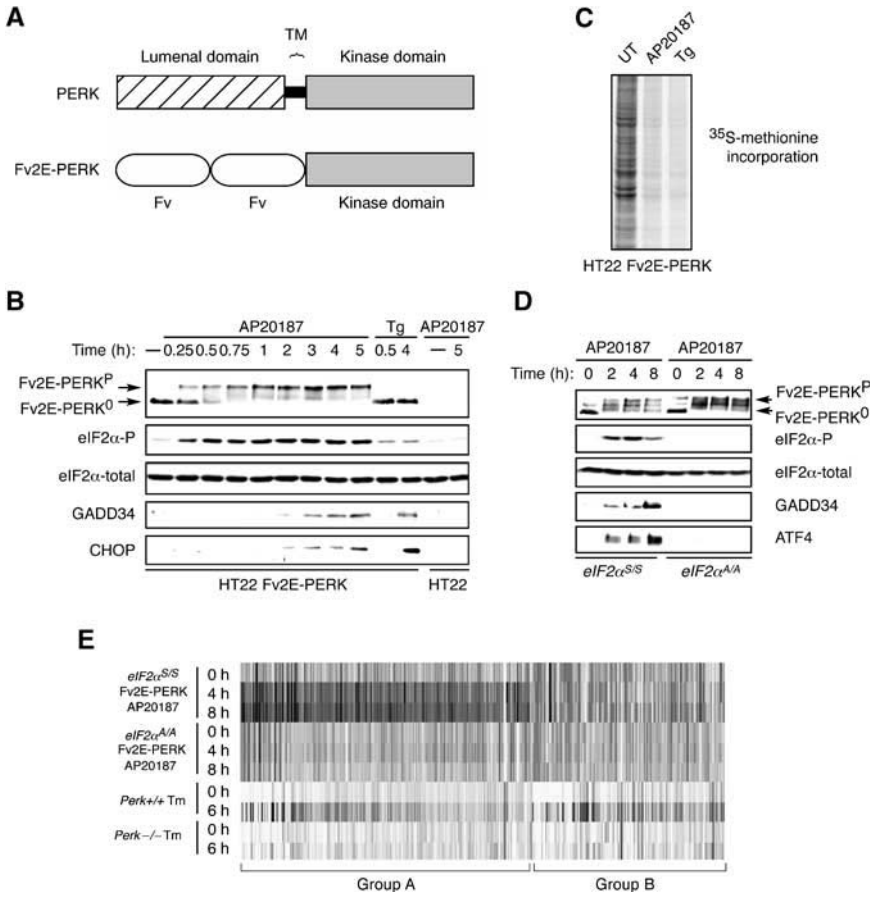

Figure 3 Uncoupling the eIF2α kinase activity of PERK from its activation by ER stress. (**A**) Schematic representation of the Fv2E-PERK fusion protein. The modified FKBP domains (Fv) and the transmembrane domain of PERK (TM) are indicated. (**B**) Immunoblot of Fv2E-PERK, phosphorylated (eIF2α-P) and total eIF2α, and the downstream targets GADD34 and CHOP in lysates of Fv2E-PERK-expressing HT22 cells and parental HT22 cells following treatment with 1 nM of the AP20187 dimerizer or thapsigargin (Tg). The position of the activated and phosphorylated (Fv2E-PERK^{P}) and the inactive hypophosphorylated Fv2E-PERK (Fv2E-PERK^{0}) are indicated. (**C**) Autoradiogram of ^{35}S-methionine incorporation into newly synthesized proteins in Fv2E-PERK-expressing HT22 cells that had been left untreated (UT) or had been treated with 1 nM AP20187 for 1 h or 400 nM thapsigargin (Tg) for 0.5 h. (**D**) Immunoblot of Fv2E-PERK, phosphorylated (eIF2α-P) and total eIF2α, and the downstream targets GADD34 and ATF4 in lysates of Fv2E-PERK-expressing MEFs with wild-type (S/S) and mutant (A/A) eIF2α genotypes, following treatment with 2 nM of the AP20187 dimerizer. (**E**) Microarray analysis of the expression level of ISR target genes in Fv2E-PERK MEFs with wild-type (S/S) and mutant (A/A) eIF2α genotypes. The 375 genes induced at least two-fold in both AP20187-treated Fv2E-PERK MEFs (at either 4 or 8 h) and tunicamycin-treated wild-type MEFs or in tunicamycin-treated MEFs alone are shown. The expression levels of the genes are shaded, with white indicating low levels of expression and black indicating high levels of expression. The genes are clustered to reveal a group of PERK-dependent tunicamycin-induced genes that are also activated by Fv2E-PERK (Group A) and a group of PERK-dependent tunicamycin-induced genes that are not induced by Fv2E-PERK activation (Group B).

HT22 cells lacking Fv2E-PERK (Figure 3B), and Fv2E-PERK does not require endogenous PERK for its activity nor does it activate endogenous PERK (see below, Figure 6B). As expected, treatment of Fv2E-PERK-expressing cells with AP20187 also results in translational inhibition demonstrated by reduced ^{35}S-methionine incorporation into newly synthesized protein. The magnitude of the reduction is similar to those observed in ER stressed cells (Figure 3C).

The Fv2E-PERK transgenic cells allowed us to survey the gene expression program activated by an eIF2α kinase under conditions in which parallel stress-induced signaling pathways were not activated. To facilitate comparison between the profiles of genes expressed in AP20187-treated Fv2E-PERK cells and a previously performed survey of the ISR (Harding *et al*, 2003), we carried out the expression microarray analysis in Fv2E-PERK containing MEFs (see below, Figure 6). The mRNA level of 506 genes was increased two-fold or more at 4 or 8 h following AP20187 treatment, compared with the untreated Fv2E-PERK positive cells (Figure 3E and Table I).

This AP20187-dependent response overlapped with the response to the ER stress-inducing drug tunicamycin. Furthermore, the overlap between the two responses substantially coincided with the portion of the ER stress response that is dependent on eIF2α phosphorylation, as it is compromised in *Perk*−/− cells (Figure 3E, Group A, Table I). This subset of genes encodes enzymes involved in amino acid metabolism, thiol metabolism and sufficiency, and resistance to oxidative and other cellular stresses (Table I): all recognized target genes of the ISR. Remarkably, many genes encoding ER chaperones and other classical targets of the ER stress response such as genes involved in protein degradation were also activated by Fv2E-PERK. The latter observations are consistent with a prominent role of eIF2α phosphorylation in controlling such classic unfolded protein response genes, which was revealed previously by analysis of

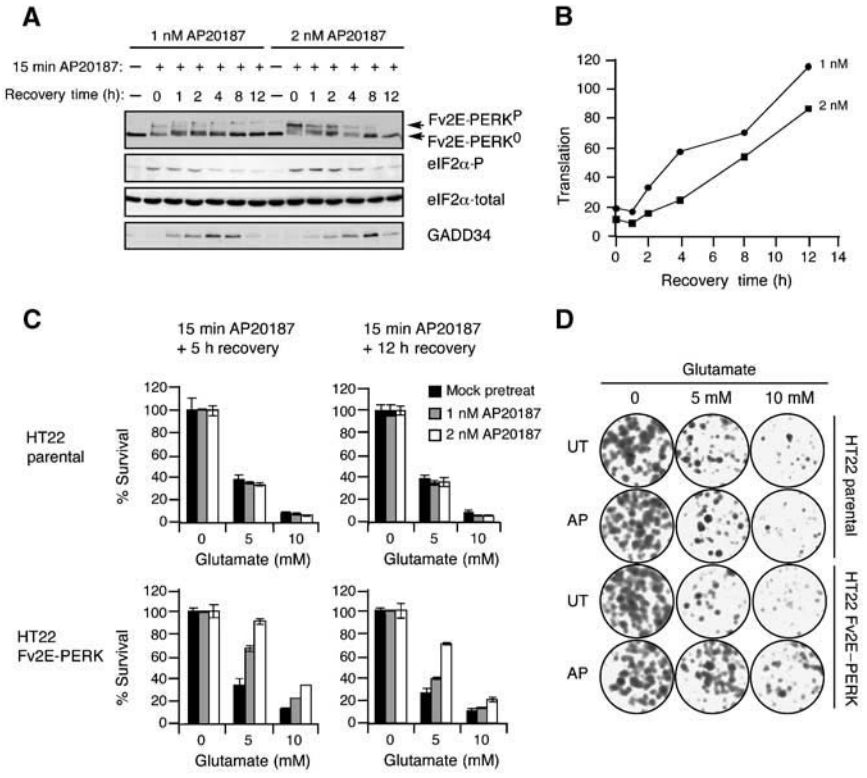

Figure 4 Activation of Fv2E-PERK enhances survival of glutamate-exposed HT22 cells. (**A**) Immunoblot of Fv2E-PERK, phosphorylated eIF2α (eIF2α-P), total eIF2α and the downstream target GADD34 in untreated cells (UT) and at various points of recovery following a 15-min exposure to 1 or 2 nM AP20187. The position of the activated Fv2E-PERK^{P} and inactive Fv2E-PERK^{0} proteins is indicated. (**B**) ^{35}S-methionine incorporation into newly synthesized proteins at various time points of recovery from translational inhibition by treatment for 15 min with 1 nM AP20187 (circles) or 2 nM AP20187 (squares). Translation is expressed as the percentage of ^{35}S-methionine incorporation into untreated cells, which is arbitrarily set at 100%. (**C**) Survival of parental HT22 cells or cells expressing Fv2E-PERK that had been treated with 1 nM, or 2 nM AP20187 or ethanol carrier for 15 min followed by 5 or 12 h of recovery and subsequently exposed to the indicated concentration of glutamate for 24 h. 100% survival is defined as the MTT reduction in cells that had not been exposed to glutamate in each AP20187 treatment group. The means ± SEM of a representative experiment performed in duplicate and repeated four times are shown. (**D**) Photomicrographs of crystal-violet-stained parental HT22 cells or cells expressing Fv2E-PERK treated with 1 or 2 nM AP20187 or ethanol carrier for 1 h followed by 5 h of recovery and subsequently exposed to glutamate for 24 h. The cells were switched to regular media for 6 days and then stained with crystal violet.

cells with mutations affecting the ISR (Scheuner *et al*, 2001; Harding *et al*, 2003) (Table I).

To determine directly the role of eIF2α phosphorylation in activated gene expression by Fv2E-PERK, we expressed the chimeric protein in fibroblasts derived from mouse embryos homozygous for a serine 51 to alanine mutation of endogenous eIF2α gene (eIF2α$^{A/A}$, the wild type being eIF2α$^{S/S}$). This mutation abolishes the phosphorylation site used by eIF2α kinases and deregulates eIF2 activity (Scheuner *et al*, 2001). Despite expressing high levels of active Fv2E-PERK, AP20187-treated eIF2α$^{A/A}$ cells have no phosphorylated eIF2α and are unable to activate the downstream targets ATF4 and GADD34 (Figure 3D). Expression microarrays showed that the cluster of genes induced by both Fv2E-PERK activation and by ER stress in wild-type (eIF2α$^{S/S}$) cells (Group A in Figure 3E) failed to undergo induction in the Fv2E-PERK-expressing mutant eIF2α$^{A/A}$ cells, thus establishing an essential role for eIF2α phosphorylation in the activation of the ISR by Fv2E-PERK.

A smaller subset of genes that were induced by ER stress but not by Fv2E-PERK activation was also identified (Figure 3E, Group B); these presumably represent targets of parallel pathways active in the ER stress response (Harding *et al*, 2002; Kaufman, 2002). A third category of genes was prominently induced by activation of Fv2E-PERK in wild-type eIF2α$^{S/S}$ cells, but less so by ER stress and not at all in mutant eIF2α$^{A/A}$ cells. Among these were genes transiently induced by Fv2E-PERK (higher at 4 h than at 8 h), a subset that may be enriched in short-lived mRNAs stabilized by translational repression, which peaks early in the AP20187-treated wild-type eIF2α$^{S/S}$ cells but is later reversed as GADD34 is induced. This mechanism of gene activation is likely to be less important in tunicamycin-treated cells, because of the gradual onset of eIF2α phosphorylation and more modest translational repression effected by that drug (Harding *et al*, 2000b). Such differences may account for the larger number of genes activated by Fv2E-PERK than by tunicamycin (data not shown and supplementary tables).

AP20187-induced Fv2E-PERK activation protects cells against oxidative glutamate toxicity, peroxynitrite donor and ER stress

Treatment of Fv2E-PERK-expressing HT22 cells with AP20187 for as little as 15 min was sufficient to induce eIF2α phosphorylation (Figures 3B and 4A). Subsequent activation of downstream gene expression was enhanced after the drug

Table I Expression level of genes induced at least two-fold at 8 h in AP20187-treated Fv2E-PERK and 1.5-fold in tunicamycin-treated wild-type (WT) cells. The expression level of the same genes in AP20187-treated Fv2E-PERK expressing mutant eIF2$\alpha^{A/A}$ cells and tunicamycin-treated Perk−/− cells is shown for comparison. The genes have been grouped into functional categories, six of which are shown here. (A complete list of all 506 genes activated at least two-fold by AP20187 treatment is provided in a supplementary table.) The mean ± average deviation of the expression level (normalized signal strength, see Methods) in untreated and treated cells from two independent experiments is shown

Name	Description	Genbank	eIF2α (S/S) Fv2E-PERK			eIF2α (A/A) Fv2E-PERK			*Perk +/+*		*Perk−/−*	
			AP20187			AP20187			Tunicamycin		Tunicamycin	
			0 h	4 h	8 h	0 h	4 h	8 h	0 h	6 h	0 h	6 h
Translation/amino acid transport and metabolism												
Myd116	EIF2alpha phosphatase, mouse GADD34	X51829	1.70 ± 0.28	9.19 ± 0.35	12.97 ± 0.82	1.05 ± 0.09	0.93 ± 0.20	1.06 ± 0.07	0.06 ± 0.29	6.90 ± 0.13	0.45 ± 0.10	0.71 ± 0.38
Abcf2	ATP-binding cassette, subfamily F2 (GCN20)	AI837318	3.97 ± 0.87	4.30 ± 0.48	8.13 ± 1.15	1.64 ± 0.01	1.70 ± 0.21	1.62 ± 0.23	0.09 ± 0.58	1.04 ± 0.04	0.59 ± 0.26	0.12 ± 0.09
Asns	Asparagine synthetase	AV253908	0.86 ± 0.15	3.90 ± 0.60	7.91 ± 1.95	1.11 ± 0.07	0.80 ± 0.01	0.94 ± 0.02	1.08 ± 0.35	2.07 ± 0.05	0.52 ± 0.04	1.29 ± 0.42
Mthfr	5,10-methylenetetrahydrofolate reductase	AW214225	1.25 ± 0.20	9.84 ± 0.94	7.78 ± 0.38	1.16 ± 0.02	1.44 ± 0.16	0.91 ± 0.26	0.68 ± 0.26	1.51 ± 0.30	0.41 ± 0.25	0.97 ± 0.57
Slc1a4	Glutamate/neutral amino acids transporter	U75215	1.96 ± 0.06	5.92 ± 0.26	6.51 ± 0.69	0.97 ± 0.02	1.32 ± 0.05	1.03 ± 0.01	0.96 ± 0.15	2.23 ± 0.71	0.16 ± 0.09	0.59 ± 0.40
Sars1	Seryl-aminoacyl-tRNA synthetase 1	AI837395	2.24 ± 0.84	3.28 ± 0.42	6.13 ± 1.07	1.37 ± 0.02	1.21 ± 0.13	1.15 ± 0.27	0.20 ± 0.29	1.80 ± 0.31	0.33 ± 0.06	0.97 ± 0.32
Cars	Cysteinyl-tRNA synthetase	AI848732	1.26 ± 0.37	5.21 ± 0.25	6.07 ± 0.89	1.11 ± 0.11	1.33 ± 0.07	1.02 ± 0.09	0.79 ± 0.26	1.95 ± 0.10	0.05 ± 0.20	0.54 ± 0.50
SYTC	Threonyl-tRNA synthetase	AI849620	1.66 ± 0.18	3.15 ± 0.00	4.74 ± 0.57	1.04 ± 0.20	1.10 ± 0.06	0.97 ± 0.02	0.80 ± 0.20	1.44 ± 0.02	0.58 ± 0.09	0.78 ± 0.34
Rps6ka2	Ribosomal protein S6 kinase, 90 kD, polypeptide 2	AJ131021	1.75 ± 0.24	3.65 ± 0.25	4.72 ± 1.01	0.90 ± 0.14	0.92 ± 0.14	0.74 ± 0.35	0.67 ± 0.29	1.80 ± 0.31	0.79 ± 0.01	0.92 ± 0.23
Lars	Leucyl-tRNA synthetase	AI844089	1.26 ± 0.17	2.35 ± 0.01	4.45 ± 0.62	1.19 ± 0.05	1.19 ± 0.01	1.10 ± 0.02	0.96 ± 0.14	1.89 ± 0.12	0.63 ± 0.03	0.92 ± 0.03
Eprs	Glutamyl-prolyl-tRNA synthetase	X54327	1.73 ± 0.34	2.28 ± 0.31	4.39 ± 0.35	1.08 ± 0.07	1.18 ± 0.12	1.32 ± 0.07	0.99 ± 0.20	1.71 ± 0.27	0.52 ± 0.04	0.76 ± 0.04
Pycs	Pyrroline-5-carboxylate synthetase	AW124889	1.86 ± 0.59	3.15 ± 0.07	4.32 ± 0.09	1.05 ± 0.08	1.04 ± 0.05	0.93 ± 0.06	0.76 ± 0.18	2.08 ± 0.14	0.56 ± 0.09	0.93 ± 0.23
Nars	Asparaginyl-tRNA synthetase	AW125874	1.76 ± 0.27	2.63 ± 0.04	4.21 ± 0.86	1.50 ± 0.07	1.44 ± 0.04	1.12 ± 0.18	0.95 ± 0.27	1.64 ± 0.22	0.64 ± 0.06	0.83 ± 0.02
WRS	Alpha-2 subunit; tryptophanyl-tRNA synthetase	X69656	2.00 ± 0.26	2.39 ± 0.17	4.06 ± 0.65	1.05 ± 0.06	1.10 ± 0.06	0.98 ± 0.02	0.73 ± 0.39	3.06 ± 0.30	0.30 ± 0.08	0.29 ± 0.10
Aars	Alanyl-tRNA synthetase	AI839392	1.73 ± 0.36	3.13 ± 0.15	4.01 ± 0.32	1.06 ± 0.06	1.05 ± 0.12	0.86 ± 0.14	0.67 ± 0.05	1.52 ± 0.06	0.60 ± 0.12	1.00 ± 0.12
Eif4ebp1	EIF4E binding protein 1	U28656	1.66 ± 0.48	2.80 ± 0.23	3.82 ± 0.56	1.02 ± 0.01	1.02 ± 0.00	0.86 ± 0.17	0.77 ± 0.14	1.55 ± 0.19	0.49 ± 0.12	0.87 ± 0.33
EST	Phosphoserine phosphatase homologue	AI846545	1.34 ± 0.22	2.54 ± 0.23	3.74 ± 0.37	1.30 ± 0.12	1.21 ± 0.09	1.12 ± 0.32	0.87 ± 0.17	1.57 ± 0.04	0.54 ± 0.07	0.96 ± 0.06
Yars	Tyrosyl-tRNA synthetase	AW122542	1.33 ± 0.56	2.85 ± 0.24	3.59 ± 0.24	1.11 ± 0.17	1.14 ± 0.13	1.03 ± 0.04	0.96 ± 0.06	1.59 ± 0.15	0.85 ± 0.11	1.08 ± 0.12
Elp3	Elongation protein 3 homolog *(S. cerevisiae)*	AI851229	1.45 ± 0.16	1.47 ± 0.28	2.91 ± 0.06	1.00 ± 0.04	1.16 ± 0.04	1.06 ± 0.03	0.26 ± 0.11	1.04 ± 0.03	0.70 ± 0.02	0.47 ± 0.01
EST	Isoleucyl-tRNA synthetase	AI848393	1.23 ± 0.15	2.30 ± 0.05	2.79 ± 0.27	0.82 ± 0.10	0.85 ± 0.14	0.75 ± 0.10	0.78 ± 0.11	1.23 ± 0.07	0.68 ± 0.03	1.00 ± 0.03
Slc1a7	Neutral amino acid transporter, ASCT2	L42115	1.16 ± 0.27	1.78 ± 0.42	2.39 ± 0.20	1.08 ± 0.24	1.11 ± 0.05	1.17 ± 0.05	0.72 ± 0.36	1.45 ± 0.00	0.11 ± 0.83	0.24 ± 0.55
Shmt2	Serine hydroxymethyl transferase 2	AV009978	1.02 ± 0.01	1.47 ± 0.01	2.34 ± 0.45	0.78 ± 0.07	0.86 ± 0.14	0.86 ± 0.06	0.70 ± 0.34	1.67 ± 0.48	0.42 ± 0.03	0.80 ± 0.77
Stress response												
EST	UVRAG homologue, UV radiation resistance	AI020259	21.66 ± 5.89	64.05 ± 9.26	49.58 ± 14.9	4.35 ± 0.05	4.89 ± 0.17	4.08 ± 0.77	0.01 ± 0.00	0.07 ± 0.37	0.10 ± 0.63	0.01 ± 0.00
Gch	GTP cyclohydrolase 1	L09737	2.98 ± 1.05	12.96 ± 1.15	21.76 ± 0.80	0.88 ± 0.16	0.68 ± 0.02	0.63 ± 0.36	0.62 ± 0.06	3.24 ± 0.91	0.93 ± 0.15	0.47 ± 0.52
GADD45	Mus musculus GADD45 protein (gadd45) gene	U00937	2.74 ± 0.06	21.42 ± 0.42	20.24 ± 0.34	1.11 ± 0.10	1.27 ± 0.10	0.92 ± 0.00	0.65 ± 0.55	10.25 ± 1.16	0.24 ± 0.06	0.44 ± 0.40
Ndr1	N-myc downstream regulated 1	U60593	5.76 ± 1.82	9.26 ± 0.70	14.09 ± 2.25	1.02 ± 0.24	1.01 ± 0.35	1.05 ± 0.35	0.67 ± 0.11	2.94 ± 0.55	0.59 ± 0.04	0.85 ± 0.47
Sqstm1	Sequestosome 1; A170, STAP	U40930	1.97 ± 0.98	4.31 ± 0.65	6.11 ± 0.59	1.21 ± 0.04	1.26 ± 0.29	1.26 ± 0.01	0.56 ± 0.17	1.74 ± 0.08	0.31 ± 0.35	0.65 ± 0.43
Arnt3	Aryl hydrocarbon receptor nuclear translocator-like	AB014494	1.18 ± 0.08	3.08 ± 0.21	3.04 ± 0.03	0.95 ± 0.09	1.06 ± 0.08	0.80 ± 0.23	0.35 ± 0.03	1.10 ± 0.10	0.56 ± 0.11	0.54 ± 0.04
Dnajb9	DnaJ (Hsp40) homolog, subfamily B, member 9	AI835630	1.00 ± 0.03	1.86 ± 0.10	2.90 ± 0.02	0.88 ± 0.19	0.91 ± 0.22	0.78 ± 0.56	0.69 ± 0.26	3.74 ± 0.28	0.17 ± 0.05	0.58 ± 0.09
Tbce	Tubulin-specific chaperone e	AI852161	1.25 ± 0.02	3.40 ± 0.03	2.82 ± 0.34	1.44 ± 0.01	1.45 ± 0.17	0.98 ± 0.31	0.70 ± 0.13	1.08 ± 0.06	0.41 ± 0.50	0.57 ± 0.45
Clcn3	Chloride channel 3	AF029347	0.77 ± 0.13	1.55 ± 0.70	1.96 ± 0.26	0.98 ± 0.13	1.20 ± 0.09	0.86 ± 0.03	0.09 ± 0.57	1.69 ± 0.06	1.04 ± 0.34	1.67 ± 0.03
Dnajc3	DnaJ (Hsp40) homolog, subfamily C, member 3, p58	U28423	0.28 ± 0.03	0.80 ± 0.00	1.06 ± 0.18	0.77 ± 0.24	0.85 ± 0.39	0.76 ± 0.05	1.24 ± 0.27	6.50 ± 1.69	0.52 ± 0.00	1.24 ± 0.07
Redox/detox												
Pon2	Paraoxonase 2; esterase; antilipid oxidation	L48514	8.21 ± 0.54	12.74 ± 1.77	17.43 ± 1.80	2.62 0.31	2.973 ± 0.09	2.180 ± 0.67	0.09 ± 0.52	0.09 ± 0.55	1.06 ± 0.92	1.67 ± 0.78
B5R.1	NADH-cytochrome B5 reductase	AI839690	2.80 ± 0.17	4.60 ± 0.26	10.00 ± 1.51	1.06 ± 0.00	1.135 ± 0.18	0.924 ± 0.40	0.98 ± 0.27	3.15 ± 0.33	0.44 ± 0.01	0.57 ± 0.18
EST	Thioredoxin-like protein HT014 homologue	AA798365	1.33 ± 0.13	3.23 ± 0.00	3.16 ± 0.34	1.90 ± 0.03	1.894 ± 0.29	1.196 ± 0.51	0.37 ± 0.07	0.75 ± 0.35	0.73 ± 0.28	0.60 ± 0.36
Txnip	Thioredoxin interacting protein	AI839138	0.88 ± 0.23	2.17 ± 0.05	2.28 ± 0.25	1.08 ± 0.03	1.307 ± 0.10	0.879 ± 0.31	0.64 ± 0.43	1.43 ± 0.26	0.40 ± 0.05	0.51 ± 0.40
Cpo	Coproporphyrinogen oxidase	D16333	0.78 ± 0.05	1.64 ± 0.02	1.83 ± 0.02	0.88 ± 0.36	1.063 ± 0.02	0.929 ± 0.18	0.95 ± 0.44	3.31 ± 0.34	0.42 ± 0.02	1.00 ± 0.11
Protein degradation												
Siah2	Seven in absentia 2; ubiquitin ligase	Z19581	1.19 ± 0.08	3.52 ± 0.09	3.45 ± 0.50	0.88 ± 0.01	0.937 ± 0.09	0.952 ± 0.05	0.80 ± 0.02	2.63 ± 0.33	0.89 ± 0.10	0.41 ± 0.49
Fbxo8	f-box only protein 8	AI844932	0.97 ± 0.45	2.34 ± 0.62	2.92 ± 0.33	2.38 0.58	1.828 ± 0.29	1.182 ± 0.26	0.69 ± 0.34	1.17 ± 0.22	0.65 ± 0.01	1.15 ± 0.09
Ctsc	Cathepsin C	U74683	1.06 ± 0.23	1.10 ± 0.01	2.24 ± 0.10	0.33 0.12	0.295 ± 0.05	0.136 ± 0.09	0.53 ± 1.15	0.84 ± 0.92	0.32 ± 0.20	0.31 ± 0.57
Secretory pathway												
Wfs1	Wolfram syndrome 1 homolog, ER localized	AF084482	2.71 ± 0.42	3.45 ± 0.15	7.75 ± 0.51	1.12 ± 0.23	1.185 ± 0.24	0.990 ± 0.26	0.06 ± 0.27	5.64 ± 0.09	0.04 ± 0.09	0.73 ± 0.05
Spaf	Transitional endoplasmic reticulum ATPase	AF016544	2.00 ± 0.28	3.12 ± 0.06	4.74 ± 0.51	1.00 ± 0.02	0.877 ± 0.11	0.728 ± 0.13	0.27 ± 0.16	0.90 ± 0.32	0.65 ± 0.18	0.34 ± 0.25
Herpud1	Homocysteine-inducible-ubiquitin-like domain 1	AI846938	1.07 ± 0.15	4.28 ± 0.19	3.11 ± 0.17	0.94 ± 0.07	0.898 ± 0.14	0.686 ± 0.17	0.38 ± 0.33	3.84 ± 0.33	0.19 ± 0.07	0.74 ± 0.17
Ero1l	Endoplasmic reticulum oxidoreductin 1-like	AA798624	1.00 ± 0.14	1.91 ± 0.26	2.59 ± 0.33	0.92 ± 0.10	1.065 ± 0.08	1.066 ± 0.23	0.52 ± 0.47	2.03 ± 0.02	0.72 ± 0.21	1.13 ± 0.12
Sel1h	Sel1 (suppressor of lin-12) 1 homologue	AW121840	0.79 ± 0.43	1.04 ± 0.30	2.19 ± 0.73	1.04 ± 0.01	0.887 ± 0.11	1.029 ± 0.12	0.77 ± 0.56	5.96 ± 4.70	0.20 ± 0.04	0.35 ± 0.12
ERO1Lb	Endoplasmic reticulum oxidoreductin 1-like-beta	AI049144	0.27 ± 0.04	0.81 ± 0.15	1.09 ± 0.02	0.77 ± 0.08	0.823 ± 0.05	0.599 ± 0.10	0.89 ± 0.26	4.02 ± 0.57	0.68 ± 0.16	1.44 ± 0.54
Transcription												
Atf3	Activating transcription factor 3	U19118	2.54 ± 0.26	24.52 ± 1.62	15.21 ± 1.69	0.92 ± 0.10	1.041 ± 0.18	0.881 ± 0.08	0.73 ± 0.08	3.35 ± 0.57	0.64 ± 0.28	0.94 ± 0.14
Nrbf1	Nuclear receptor binding factor 1	AW046483	4.30 ± 0.56	4.74 ± 0.55	8.75 ± 0.11	2.41 ± 0.26	2.378 ± 0.24	1.855 ± 0.87	0.03 ± 0.06	1.68 ± 1.71	0.11 ± 0.80	0.06 ± 0.28
Nfkb2	Nuclear factor of kappa B cell 2	AW047899	3.27 ± 0.23	6.45 ± 0.32	8.26 ± 1.04	0.99 ± 0.01	0.971 ± 0.13	1.043 ± 0.08	0.38 ± 0.09	0.80 ± 0	0.94 ± 0.11	0.86 ± 0.15
Atf5	Activating transcription factor 5	AB012276	2.22 ± 0.27	5.79 ± 0.26	7.54 ± 2.44	1.36 ± 0.04	1.365 ± 0.33	1.050 ± 0.13	0.99 ± 0.21	2.80 ± 0.56	0.23 ± 0.12	0.37 ± 0.35
Chop-10	Transcription factor CHOP, GADD153	X67083	0.98 ± 0.08	4.35 ± 0.65	6.41 ± 0.25	1.10 ± 0.27	1.176 ± 0.15	0.940 ± 0.19	0.60 ± 0.34	11.30 ± 0.07	0.49 ± 0.05	0.75 ± 0.27
Nupr1	Nuclear protein 1	AI852641	1.36 ± 0.23	5.85 ± 0.47	6.29 ± 1.64	1.26 ± 0.17	1.449 ± 0.32	1.119 ± 0.16	1.22 ± 0.75	3.37 ± 0.39	0.02 ± 0.01	0.59 ± 0.25
Cebpg	CCAAT/enhancer binding protein (C/EBP), gamma	AB012273	1.94 ± 0.22	6.31 ± 0.39	5.96 ± 0.12	1.07 ± 0.03	1.068 ± 0.01	0.906 ± 0.07	0.89 ± 0.25	1.75 ± 0.09	0.52 ± 0.29	0.60 ± 0.19
Relb	(v-rel) oncogene related B	M83380	2.60 ± 0.02	9.02 ± 0.60	5.87 ± 1.42	0.90 ± 0.07	1.054 ± 0.09	1.182 ± 0.27	0.56 ± 0.21	1.00 ± 0.41	0.68 ± 0.09	0.68 ± 0.00
Tbpl1	TATA box binding protein-like 1	AB017697	1.79 ± 0.17	3.42 ± 0.11	5.63 ± 0.45	1.89 ± 0.27	2.069 ± 0.05	1.415 ± 0.53	0.55 ± 0.47	1.08 ± 0.08	0.55 ± 0.20	0.54 ± 0.13
Cebpb	CCAAT/enhancer binding protein (C/EBP), beta	M61007	2.10 ± 0.37	3.31 ± 0.41	4.23 ± 0.68	1.02 ± 0.03	0.952 ± 0.07	1.099 ± 0.30	0.98 ± 0.30	1.96 ± 0.05	0.48 ± 0.02	0.55 ± 0.13
Cbx4	Chromobox homolog 4, transcriptional repressor	U63387	1.48 ± 0.37	3.07 ± 0.08	4.16 ± 0.88	1.17 ± 0.03	1.111 ± 0.23	1.107 ± 0.10	0.91 ± 0.10	1.98 ± 0.41	0.61 ± 0.19	0.91 ± 0.01
SKiP	Ski-interacting protein, nuclear receptor coactivator	AW046671	1.91 ± 0.60	2.84 ± 0.23	3.87 ± 0.09	1.16 ± 0.01	1.319 ± 0.28	0.973 ± 0.13	0.55 ± 0.22	1.15 ± 0.20	0.75 ± 0.11	0.65 ± 0.17
ATF6	ATF6 alpha homologue	AA592069	1.32 ± 0.30	2.05 ± 0.24	3.85 ± 0.81	0.83 ± 0.39	0.979 ± 0.15	1.059 ± 0.14	0.30 ± 0.14	1.86 ± 0.01	0.48 ± 0.07	0.30 ± 0.08
Atf4	Activating transcription factor 4	M94087	1.62 ± 0.13	3.01 ± 0.18	3.60 ± 0.61	0.85 ± 0.08	1.012 ± 0.02	1.045 ± 0.06	0.84 ± 0.02	1.80 ± 0.02	0.52 ± 0.15	0.99 ± 0.19
Nfil3; E4BP	NFIL3/E4BP4 transcription factor	U83148	1.51 ± 0.13	4.29 ± 0.49	3.56 ± 0.37	0.87 ± 0.16	0.927 ± 0.19	0.756 ± 0.31	0.60 ± 0.09	1.92 ± 0.08	0.28 ± 0.03	0.29 ± 0.01
Lmo4	LIM only 4; transcriptional regulator cofactor	AF074600	0.94 ± 0.27	2.98 ± 0.06	3.47 ± 0.15	1.16 ± 0.32	1.108 ± 0.21	0.976 ± 0.20	0.41 ± 0.07	1.18 ± 0.54	0.24 ± 0.24	0.31 ± 0.06
Klf4	Kruppel-like factor 4 (gut)	U20344	1.17 ± 0.02	3.58 ± 0.03	2.74 ± 0.02	0.97 ± 0.01	1.070 ± 0.07	0.770 ± 0.08	0.85 ± 0.43	1.82 ± 0.55	0.24 ± 0.33	0.35 ± 0.49
Xbp1	X-box binding protein 1	AW123880	1.00 ± 0.06	2.64 ± 0.32	2.65 ± 0.29	1.07 ± 0.06	0.950 ± 0.03	0.735 ± 0.19	0.63 ± 0.14	1.14 ± 0.12	0.12 ± 0.01	0.36 ± 0.00
Ets2	E26 avian leukemia oncogene 2, 3′ domain	J04103	1.22 ± 0.38	2.17 ± 0.28	2.41 ± 0.38	1.00 ± 0.06	1.028 ± 0.22	0.881 ± 0.10	0.66 ± 0.04	1.49 ± 0.17	0.37 ± 0.18	0.28 ± 0.01
Rxrip110	Retinoid X receptor interacting protein 110	U22015	0.68 ± 0.12	1.52 ± 0.07	1.74 ± 0.49	1.01 ± 0.01	1.013 ± 0.01	0.888 ± 0.11	0.53 ± 0.18	1.19 ± 0.10	0.97 ± 0.10	1.17 ± 0.71

Genes induced at least 2-fold at 8 h in AP20187 treated Fv2e-PERK and 1.5-fold in tunicamycin treated wildtype (WT) cells. The genes have been grouped into functional categories six of which are shown here. (A complete list of all 506 genes activated at least two-fold by AP20187 treatment is provided in Supplementary tables 1 and 2). The mean ± the average deviation of the normalized signal from treated to untreated cells from two independent experiments is shown.

was withdrawn, as translation rates were recovering (Figure 4A and B). Thus, a short pulse of AP20187 followed by withdrawal of the drug mimics the kinetic profile of a response of cells to stress (Brostrom and Brostrom, 1998; Novoa *et al*, 2003). Therefore, cells were exposed to AP20187 for 15 min, the dimerizer was removed and, following a variable recover period of 5 or 12 h, the cells were exposed to glutamate. AP20187 pretreatment protected Fv2E-PERK-expressing HT22 cells from subsequent exposure to glutamate, but did not affect the survival of parental HT22 cells (Figure 4C and D). The survival advantage of pretreatment correlated with the dose of dimerizer used and was still apparent 12 h after withdrawal of the dimerizer, a point at which translation had recovered to nearly normal levels (Figure 4B).

Oxidative glutamate toxicity is attributed to inhibited import of cystine and consequent glutathione depletion, resulting in accumulation of endogenous peroxides (Murphy *et al*,

1989). To determine if eIF2α phosphorylation affects the development of oxidative stress or acts downstream of it, we measured levels of endogenous peroxides induced by glutamate using dichlorofluorescin (DCF), a cell-permeant molecule that is oxidized by endogenous peroxides and other oxidants to the fluorescent dichlorofluoresceine. AP20187 had no measurable effect on DCF fluorescence in parental HT22 cells (Figure 5A and B) whereas glutamate treatment resulted in a profound increase in DCF fluorescence as detected by FACscan (Figure 5C and D). DCF fluorescence levels fell only when the cells died, an event reflected by permeability to propidium iodide (Figure 5 A–D).

AP20187 pretreatment of Fv2E-expressing cells did not affect DCF fluorescence in cells that were not exposed to glutamate (Figure 5E and F), but markedly reduced DCF fluorescence in the cells exposed to glutamate (Figure 5G and H). Treatment with AP20187 caused some death among the Fv2E-PERK-expressing cells (compare the upper left quadrants in Figure 5E and F), as predicted by the pro-apoptotic effects of another eIF2α kinase PKR (Srivastava *et al*, 1998). However, in cells exposed to glutamate, AP20187 dramatically reduced the fraction of propidium iodide positive (dead) cells (compare the upper left quadrants in Figure 5G and H). AP20187 pretreatment also protects against glutamate-induced glutathione depletion (Figure 5I). The latter observation links the protective effect of the eIF2α phosphorylation induced by Fv2E-PERK to the previously established role of oxidative glutamate toxicity in glutathione depletion (Tan *et al*, 1998a). These experiments show that activation of an eIF2α kinase prevents oxidative stress and cell death in HT22 cells exposed to glutamate.

To measure the effect of Fv2E-PERK activation on the sensitivity of cells to other stressful conditions, we introduced the transgene into immortalized mouse embryo fibroblasts, which are sensitive to both ER stress and nitrosative stress. In these cells too, AP20187 treatment activated Fv2E-PERK, phosphorylated eIF2α and activated downstream genes. This is apparent in wild-type cells and even more so in *Perk−/−* cells which, lacking the endogenous eIF2α kinase activity, were able to tolerate higher levels of Fv2E-PERK (Figure 6A and B). AP20187 protected the Fv2E-PERK transgenic cells with a wild-type eIF2α genotype ($eIF2\alpha^{S/S}$) against the lethal effects of the ER stress-inducing agent tunicamycin and the peroxinitrite donor SIN-1 (Figure 6C and D). No protection was afforded by AP20187 to the Fv2E-PERK transgenic cells with the serine 51 to alanine mutation in eIF2α ($eIF2\alpha^{A/A}$).

Discussion

Phosphorylation of eIF2α impacts on the cell at two levels: it reduces the rate of translation initiation and with it protein

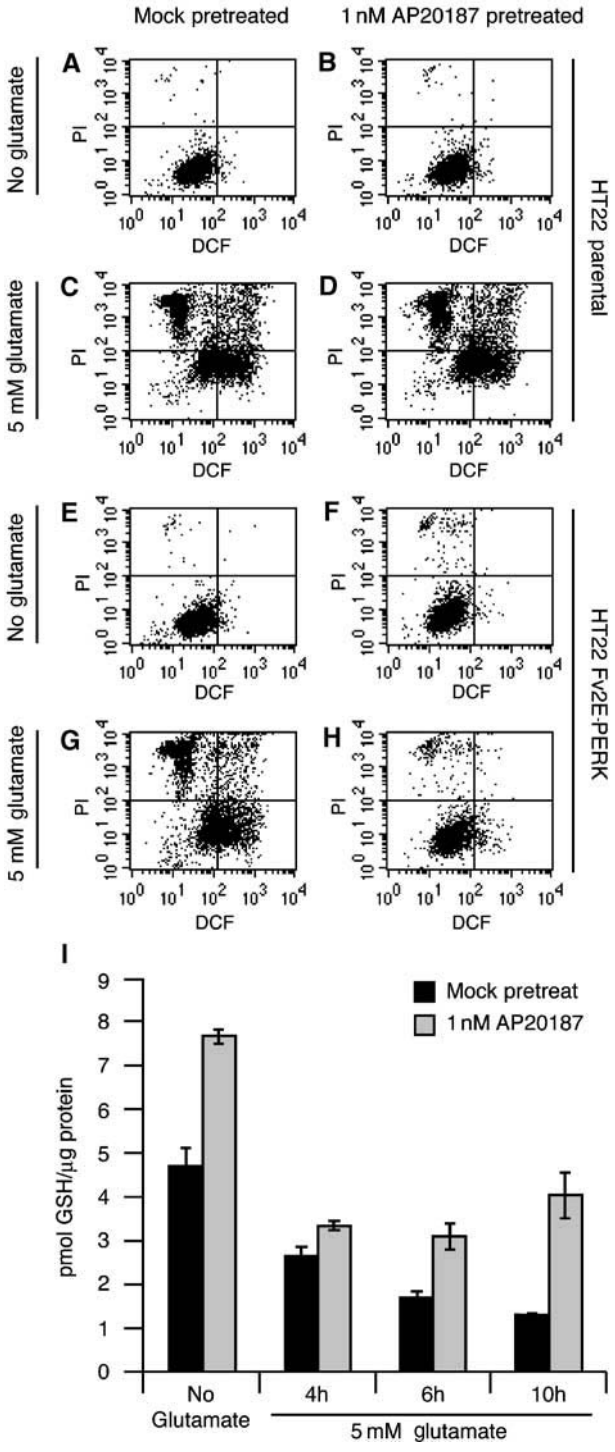

Figure 5 AP20187-mediated activation of Fv2E-PERK reduces the levels of glutamate-induced endogenous peroxides and rescues glutamate-induced glutathione depletion. Dual-channel FACscans of dichlorofluorescein fluorescence (*X*-axis) and propidium iodide fluorescence (*Y*-axis) of parental HT22 cells (**A**–**D**) or Fv2E-PERK cells (**E**–**H**) that were either mock pretreated (**A**, **C**, **E**, **G**) or pretreated with 1 nM AP20187 for 1 h followed by a 5 h recovery period (**B**, **D**, **F**, **H**) before exposure to 5 mM glutamate for 10 h (**C**, **D**, **G**, **H**) are shown. The fraction of cells in each quadrant of the two-dimensional FACscan is displayed in the table below.

	A (%)	B (%)	C (%)	D (%)	E (%)	F (%)	G (%)	H (%)
Upper lt	0.78	1.23	32.53	32.86	1.28	5.93	33.61	7.39
Upper rt	0.09	0.19	15.44	16.31	0.17	0.23	8.10	0.73
Lower lt	97.31	96.35	27.14	23.87	95.84	92.92	28.45	87.26
Lower rt	1.82	2.24	24.90	26.96	2.72	0.92	29.84	4.62

(I) Glutathione levels in HT22 cells expressing Fv2E-PERK either mock pretreated or pretreated with 1 nM AP20187 followed by a 5 h recovery period. Glutathione levels were measured at various points after exposure to 5 mM glutamate or at 10 h postrecovery in the absence of glutamate. The means ± SEM ($n = 2$) are shown.

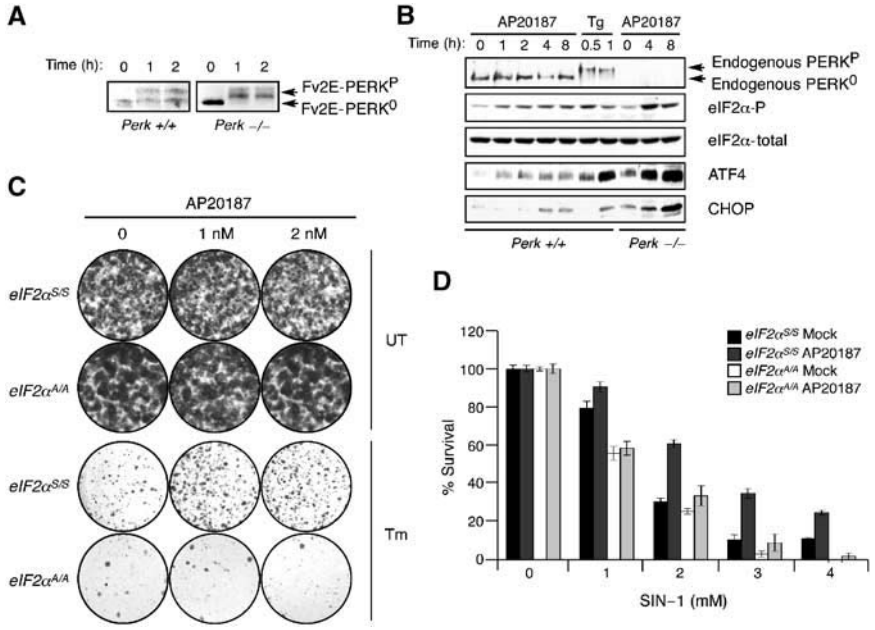

Figure 6 AP20187-induced activation of Fv2E-PERK in MEFs is protective against ER stress and nitrosylation stress. (**A**) Immunoblot of Fv2E-PERK from Wildtype (*Perk*+/+) and *Perk*−/− cells selected for stable expression of Fv2E-PERK and treated with 1 nM AP20187 for the indicated periods of time. The positions of the activated and phosphorylated (Fv2E-PERK^P) and the inactive hypophosphorylated Fv2E-PERK (Fv2E-PERK^0) are indicated. (**B**) Immunoblot analysis of immunoprecipitated endogenous PERK, phosphorylated eIF2α (eIF2α-P), total eIF2α, ATF4, and CHOP from *Perk*+/+ and *Perk*−/− cells expressing Fv2E-PERK and treated with 1 nM AP20187 or 400 nM thapsigargin (Tg). The positions of the activated and phosphorylated (endogenous PERK^P) and the inactive hypophosphorylated PERK (endogenous PERK^0) are indicated. (**C**) Photomicrographs of crystal-violet-stained cells with wild-type (S/S) or mutant (A/A) eIF2α genotypes expressing Fv2E-PERK treated with AP20187 or ethanol carrier prior to exposure to tunicamycin (Tm) for 16 h as described in Methods. The media were replaced after tunicamycin exposure and the cells were stained with crystal violet 6 days later. (**D**) Survival of cells with wild-type (S/S) or mutant (A/A) eIF2α genotypes expressing Fv2E-PERK that had been pretreated with 1 nM AP20187 or ethanol carrier and exposed to SIN-1 at the indicated concentrations. 100% survival is defined as the MTT reduction in cells that had not been exposed to SIN-1. The means±SEM of a representative experiment performed in triplicate and repeated twice are shown.

synthesis while at the same time activating a gene expression program, which we refer to as the ISR. Both effects may contribute to cytoprotection. By blocking new protein synthesis, eIF2α phosphorylation may conserve energy, divert cysteine, glycine and glutamate to glutathione biosynthesis, and potentially prevent the synthesis of pro-apoptotic proteins. Indeed the protein synthesis inhibitor cycloheximide has been shown to protect neuronal cells from glutamate (Tan *et al*, 1998a, b). However, translational repression is not the only mechanism by which eIF2α phosphorylation promotes resistance to glutamate, as transient Fv2E-PERK activation is able to protect cells against glutamate exposure even when the latter occurs after phosphorylated eIF2α has fallen to basal levels and protein synthesis has recovered (Figure 4).

The target genes of the ISR include membrane transporters for cystine and glycine, as well as several enzymes involved in glutathione biosynthesis. EIF2α phosphorylation and activation of the ISR is therefore likely to reduce levels of reactive oxygen species by promoting the capacity of cells to synthesize glutathione. This conclusion is supported by higher levels of glutathione found in AP20187-treated Fv2E-PERK cells (Figure 5I) and by the observation that a mutation that stably reduces eIF2α levels in HT22 cells increases levels of γ-glutamyl cysteine synthetase, a key enzyme in glutathione biosynthesis (Tan *et al*, 2001). Several other oxidative stress response genes are also targets of the ISR (Harding *et al*, 2003) and are activated by Fv2E-PERK (Table I). As reactive oxygen species play a role in cell death in glutamate toxicity, ER stress and nitrosative stress, the persistent survival benefit afforded to HT22 cells, 12 h after transient activation of Fv2E-PERK, is likely to be mediated by the gene products of the ISR.

Levels of phosphorylated eIF2α are comparable in cells following activation of Fv2E-PERK and exposure to tunicamycin or thapsigargin (Figures 1B and 3B), and pretreatment with the stress-inducing agents provides similar levels of resistance to glutamate (compare Figures 1A and 4C). Furthermore, inhibiting eIF2α phosphorylation by overexpression of a phosphatase (GADD34) sensitizes HT22 cells to glutamate. Together these observations suggest that the ISR is an important component of heterologous preconditioning against oxidative glutamate toxicity. It is formally possible that some of the benefits accrued by activating Fv2E-PERK are mediated by pathways independent of the ISR and that GADD34 overexpression has additional sensitizing effects that are independent of eIF2α dephosphorylation. However, we regard these unlikely possibilities because PERK has no other known substrates, and a mutation in eIF2α that prevents it from being phosphorylated abolishes the effects of Fv2E-PERK activation.

Not all the target genes of the ISR promote cell survival. *CHOP*, a well-characterized target of the ISR, contributes to the susceptibility to cell death, as its overexpression kills cells (McCullough *et al*, 2001) and its deletion protects from cell death (Zinszner *et al*, 1998). Activation of such death-promoting ISR targets may account for the weak toxicity of Fv2E-PERK activation revealed in Figure 5F. Furthermore, translational inhibition, which is inherent to eIF2α phosphorylation, is incompatible with normal physiological activity and

persistent suppression of protein synthesis may also contribute to cell death caused by Fv2E-PERK activation. It is interesting however that persistent activation of the ISR is tolerated for extended periods in the context of hibernation, a physiologically quiescent stress-resistant state (Frerichs *et al*, 1994, 1998).

The data presented in this paper indicate that activation of pathways downstream of eIF2α phosphorylation may be protective against diverse conditions associated with oxidative stress. Therefore, pharmacological agents that promote eIF2α phosphorylation without adding to cell stress may be useful in a wide range of clinical situations in anticipation of cellular injury. By effecting an artificial hibernation-like stress-resistant state, drugs based on this physiological principle may be used to prevent cell injury in a variety of clinical contexts. These include post-cardiac bypass neurological injury, stroke-in-evolution, head trauma and possibly preserve peripheral organs during procurement for transplantation.

Methods

Cell culture and generation of stable cell lines

The HT22 subclone of HT-4 cells were a kind gift of Pamela Maher, and were maintained at approximately 50% confluence in regular media consisting of DMEM (Life Science Technologies), 10% fetal calf serum (FCS, Atlanta Biologicals), 1 × pen/strep and 2 mM L-glutamine (Life Science Technologies) as described (Maher and Davis, 1996). *Wildtype*, *Perk−/−* and *eIF2α*$^{A/A}$ MEFs immortalized with SV40 large T antigen were grown in the same medium (Harding *et al*, 2000b; Scheuner *et al*, 2001).

Cells expressing active GADD34 were produced by transducing HT22 cells with pBabe, a retrovirus encoding the active A1 fragment of hamster GADD34 (Novoa *et al*, 2001). GADD34$^{\Delta C}$-overexpressing cells were made by transducing HT22 cells with retrovirus encoding the inactive GADD34 mutant lacking the C-terminal 121 amino acids, which contain the domain required for binding the catalytic subunit of the phosphatase. The transduced HT22 cells were selected for stable expression of the GADD34 fragments with 4 μg/ml puromycin (Calbiochem) and maintained in regular media supplemented with 55 μM βME and 1 × MEM non-essential amino acids (NEAA) from Life Technologies. The level of expression of the active A1 fragment of GADD34 in pools of transduced cells used in these experiments was similar to that observed previously and is estimated to be several fold higher than the endogenous levels in stressed cells (Novoa *et al*, 2001).

The use of FK506 binding domains to create drug-activated fusion proteins has previously been described (Spencer *et al*, 1993). A modified version of the FK506 binding domain has recently been engineered to bind specifically to a synthetic dimerization-inducing ligand, AP20187, which is incapable of interacting with endogenous FK506 binding proteins (www.ariad.com/regulationkits). The Fv2E-PERK construct was made using the ARIAD Regulated Homodimerization Kit. Briefly, the portion of the mouse *Perk* cDNA encoding the kinase domain kinase domain (amino acids 537–1114) was fused to two tandem modified FK506 binding domains (Fv2E) from the pC_4M-Fv2E plasmid. The 5′ myristoylation signal encoded in pC_4M-Fv2E was removed and the Fv2E-PERK transgene was shuttled into a retroviral vector, pBabe (Morgenstern and Land, 1990), and used to produce replication-defective retrovirus as previously described (Landau and Littman, 1992). HT22 cells, Wildtype MEFs, *Perk−/−* MEFs and eIF2α$^{A/A}$ MEFs were transduced with pBabe retrovirus encoding Fv2E-PERK, plated to clonal dilution, and selected for stable expression of the transgene by the addition of 4 and 2.5 μg/ml puromycin, respectively. Levels of Fv2E-PERK were consistently higher in pools of transduced *Perk−/−* MEFs and eIF2α$^{A/A}$ MEFs than in the wild-type MEFs and the mutant cells stably express the transgene at high levels, whereas the wild-type cells tend to lose expression over time. These observations may reflect low levels of basal activity of the chimeric kinase (leak), which is well tolerated by cells lacking endogenous kinase activity (*Perk−/−*) and in cells with a mutant target (eIF2α$^{A/A}$) but is poorly tolerated by the wild-type cells. Several cell lines expressing equal levels of Fv2E-PERK were established from the clonal populations and these were used in the functional studies shown in Figures 3 and 6. All the assays described in this manuscript were performed in at least two different Fv2E-PERK cell lines and in the parental cells. The data shown in the figures are from representative cell lines.

Survival assays

Cells were plated at a density of $2.5–5.0 \times 10^3$ cells/96-well plate or $1.5–3.0 \times 10^4$ cells/24-well plate. After pretreatment with AP20187 (ARIAD) or mock pretreatment with an equal volume of the carrier ethanol, HT22 cells were washed once in regular media and then maintained in regular media for the duration of recovery. Following the recovery period, the media were replaced with fresh media containing L-glutamic acid (Sigma) for 24 h. MEFs were mock pretreated or pretreated for 18 h with AP20187 and then exposed to 3-morpholinosydnonimine (SIN-1, Sigma) for 6 h. The cells were switched to media containing 0.5 mg/ml MTT (3-[4,5-dimethylthiazol-2-yl]-2,5-diphenyl tetrazolium bromide, Sigma) for 4 h and the reaction was stopped by the addition of an equal volume of stop buffer (50% isopropanol, 10% SDS, 10 μM HCl). The formazan crystals were allowed to dissolve during a 16 h incubation at 37°C and the optical density was read at 550 nm. Experiments were performed in duplicate or triplicate and repeated twice.

For the colony outgrowth assay, HT22 cells were plated at a density of 1×10^3 cells/6-well plate and maintained for 6 days in non-supplemented media or media supplemented with 55 μM βME. MEFs were plated at a density of 5×10^3 cells/6 well plate and pre-treated with 1 nM AP20187 for 7 h, at which time tunicamycin was added for an additional 16 h (0.25 μg/ml for wild type, eIF2α$^{S/S}$ cells and 0.025 μg/ml for the mutant eIF2α$^{A/A}$ cells). The cells were allowed to recover and resume growth and were fixed with 4% formaldehyde 6 days later prior to staining with crystal violet. The data shown are representative wells from experiments repeated four times.

Array analysis

Two independently isolated Fv2E-PERK-expressing *Perk−/−* transformed MEF cell pools of each treatment group (0, 4, or 8 h with 2 nM AP20187) were used to isolate total RNA using the guanidine thiocyanate–acid–phenol extraction method. The use of *Perk−/−*, *Fv2E-PERK(+)* cells was favored because of the higher level of Fv2E-PERK expression. The comparison group consisted of mutant eIF2α$^{A/A}$ cells expressing comparable levels of Fv2E-PERK (Figure 3D). Fluorescent labeled RNA probes for each of the samples were prepared and hybridized to Affymetrix mouse U74Av2 high-density oligonucleotide arrays as previously described (Lockhart *et al*, 1996). Primary image analysis of the arrays was performed using the Genechip 3.2 software package (Affymetrix, Santa Clara, CA). The raw data from the hybridization experiments were analyzed by GeneSpring™. The raw signal strength from each gene was normalized to the mean signal strength of all genes from the same chip to obtain the normalized signal strength. Then, to allow visualization of all data on the same scale for subsequent analysis, the normalized signal strength of each gene was divided by the median signal strength for that gene among all samples to obtain the normalized expression level. The data were compared to the results obtained from previously published data from wild type, *Perk−/−* or *Atf4−/−* untreated or tunicamycin-treated samples (Harding *et al*, 2003). Genes that were assigned a 'present' signal flag (Genechip 3.2 software) in 8 h AP20187-treated Fv2E-PERK samples or tunicamycin-treated wild-type cells and that had a raw signal strength of greater than 50 in tunicamycin-treated wild-type cells were further analyzed. In all, 653 genes that were induced two-fold by either 4 or 8 h of AP20187 treatment of Fv2E-PERK cells or by 6 h of tunicamycin treatment in wild-type fibroblasts were identified; 506 of these were induced at least two-fold by AP20187 treatment in Fv2E-PERK cells and the remainder were induced by at least two-fold in tunicamycin-treated wild-type cells and to varying degrees in Fv2E-PERK cells (see Supplementary tables). The complete data set has been submitted to the NCBI GEO database Accession GDSH05.

Immunoblotting and translation assays

For analysis of Fv2E-PERK, eIF2α, ATF4, GADD34 and CHOP by immunoblotting 6×10^5 cells were plated onto 10 cm dishes

16 h prior to treatment. Cell extracts were prepared using harvest buffer (10 mM HEPES pH 8.0, 50 mM NaCl, 0.5 M sucrose, 0.1 M EDTA, 0.5% Triton X-100) containing both protease inhibitors (1 mM dithiothreitol (DTT), 2 μg/ml pepstatin, 4 μg/ml aprotinin, 100 μM PMSF) and phosphatase inhibitors (10 mM tetrasodium pyrophosphate, 100 mM NaF, 17.5 mM β-glycerophosphate). The low-speed supernatant (1000 g) containing cytoplasmic proteins was collected and nuclear extracts were made by vortexing the nuclei for 15 min at 4°C in buffer containing 20 mM HEPES pH 7.9, 400 mM NaCl, 1 mM EDTA, 1 mM EGTA, 0.1% IGEPAL CA-630, plus protease inhibitors. Equal amounts of protein were loaded per lane in SDS–PAGE gels (30–50 μg of cytoplasmic extract, 20 μg of nuclear extract). Immunoprecipitation procedures for detecting endogenous PERK and immunoblotting procedures for PERK, eIF2α, ATF4, GADD34 and CHOP have previously been described (Bertolotti *et al*, 2000; Harding *et al*, 2000a, b; Novoa *et al*, 2001).

To measure new protein synthesis, cells were labeled for 10 min with 50 μCi/ml ^{35}S-Translabel (ICN) in pulse media (90% DMEM without methionine and cysteine, 10% regular DMEM, 5% dialyzed FCS, 1 × pen/strep, 2 mM L-glutamine). The dishes were flooded with ice-cold PBS containing 1 mM cycloheximide, 0.6 mg/ml L-methionine and 0.96 mg/ml L-cysteine, washed twice in PBS, and harvested in 1% Triton X-100-containing buffer as described previously (Harding *et al*, 2000b). In all, 15 μg of protein/lane was loaded onto a 9% gel for detection of ^{35}S-methionine incorporation by autoradiography and 25 μg of protein/lane was loaded for detection of Fv2E-PERK, eIF2α and GADD34 by immunoblot.

Assays for endogenous peroxides and glutathione

Parental HT22 and Fv2E-PERK-expressing cells were plated at 1×10^5 cells/60 mm dish and pretreated for 1 h with 1 nM AP20187 and allowed to recover in regular media for 5 h prior to the addition of 5 mM glutamate for 10 h. The media were removed to collect floating cells and pooled with cells trypsinized from the dishes. The cells were pelleted and resuspended in fresh media containing 10 μM 2′,7′-dichloro-dihydrofluorescin diacetate (DCF, Molecular Probes) and incubated for 15 min at 37°C. Cells were then pelleted, washed once in ice-cold PBS–2% FCS, and resuspended in PBS–2% FCS containing 1 μg/ml propidium iodide (PI, Roche). After a 5-min incubation on ice, the cells were analyzed for DCF fluorescence (FL-1, green channel) and PI positivity (FL-3, red channel) by a Becton Dickson FACScan. In all, 10 000 ungated cells were counted.

Glutathione levels were measured using the modified DTNB-GSSG reductase recycling assay (Griffith, 1980; Anderson, 1985).

Supplementary data

Supplementary data are available at *The EMBO Journal* Online.

Acknowledgements

We thank ARIAD Pharmaceuticals and Vic Rivera for supplying the Fv2E expression vector and the AP20187 dimerizer drug, and Pam Maher for the HT22 cells. This work was supported by NIH grants ES08681 and DK47119 to DR and DK42394 to RJK. DR is an Ellison Medical Foundation Senior Scholar in Aging.

References

Anderson ME 1985 Determination of glutathione and glutathione disulfide in biological samples. *Methods Enzymol* **113:** 548–555

Bertolotti A, Zhang Y, Hendershot L, Harding H, Ron D 2000 Dynamic interaction of BiP and the ER stress transducers in the unfolded protein response. *Nat Cell Biol* **2:** 326–332

Brostrom CO, Brostrom MA 1998 Regulation of translational initiation during cellular responses to stress. *Prog Nucleic Acid Res Mol Biol* **58:** 79–125

Chen J 2000 Heme-regulated eIF2α kinase. In *Translational Control of Gene Expression*, Sonenberg N, Hershey JWB, and Mathews MB (eds) pp 529–546. Cold Spring Harbor: CSHL Press

Davis JB, Maher P 1994 Protein kinase C activation inhibits glutamate-induced cytotoxicity in a neuronal cell line. *Brain Res* **652:** 169–173

DeGracia DJ, Kumar R, Owen CR, Krause GS, White BC 2002 Molecular pathways of protein synthesis inhibition during brain reperfusion: implications for neuronal survival or death. *J Cereb Blood Flow Metab* **22:** 127–141

Dever TE 2002 Gene-specific regulation by general translation factors. *Cell* **108:** 545–556

Frerichs KU, Hallenbeck JM 1998 Hibernation in ground squirrels induces state and species-specific tolerance to hypoxia and aglycemia: an *in vitro* study in hippocampal slices. *J Cereb Blood Flow Metab* **18:** 168–175

Frerichs KU, Kennedy C, Sokoloff L, Hallenbeck JM 1994 Local cerebral blood flow during hibernation, a model of natural tolerance to 'cerebral ischemia'. *J Cereb Blood Flow Metab* **14:** 193–205

Frerichs KU, Smith CB, Brenner M, DeGracia DJ, Krause GS, Marrone L, Dever TE, Hallenbeck JM 1998 Suppression of protein synthesis in brain during hibernation involves inhibition of protein initiation and elongation. *Proc Natl Acad Sci USA* **95:** 14511–14516

Griffith OW 1980 Determination of glutathione and glutathione disulfide using glutathione reductase and 2-vinylpyridine. *Anal Biochem* **106:** 207–212

Harding H, Novoa I, Zhang Y, Zeng H, Wek RC, Schapira M, Ron D 2000a Regulated translation initiation controls stress-induced gene expression in mammalian cells. *Mol Cell* **6:** 1099–1108

Harding H, Zeng H, Zhang Y, Jungreis R, Chung P, Plesken H, Sabatini D, Ron D 2001 Diabetes mellitus and exocrine pancreatic dysfunction in Perk−/− mice reveals a role for translational control in survival of secretory cells. *Mol Cell* **7:** 1153–1163

Harding H, Zhang Y, Bertolotti A, Zeng H, Ron D 2000b *Perk* is essential for translational regulation and cell survival during the unfolded protein response. *Mol Cell* **5:** 897–904

Harding H, Zhang Y, Zeng H, Novoa I, Lu P, Calfon M, Sadri N, Yun C, Popko B, Paules R, Stojdl D, Bell J, Hettmann T, Leiden J, Ron D 2003 An integrated stress response regulates amino acid metabolism and resistance to oxidative stress. *Mol Cell* **11:** 619–633

Harding HP, Calfon M, Urano F, Novoa I, Ron D 2002 Transcriptional and translational control in the mammalian unfolded protein response. *Annu Rev Cell Dev Biol* **18:** 575–599

Hinnebusch AG 2000 Mechanism and regulation of initiator methionyl-tRNA binding to ribosomes. In *Translational Control of Gene Expression*, Sonenberg N, Hershey JWB, Mathews MB (eds) pp 185–243. Cold Spring Harbor: CSHL Press

Kaufman RJ 2000 The double-stranded RNA-activated protein kinase PKR. In *Translational Control of Gene Expression*, Sonenberg N, Hershey JWB, Mathews MB (eds) pp 503–527. Cold Spring Harbor: CSHL Press

Kaufman RJ 2002 Orchestrating the unfolded protein response in health and disease. *J Clin Invest* **110:** 1389–1398

Kumar R, Azam S, Sullivan J, Owen C, Cavener D, Zhang P, Ron D, Harding H, Chen J, Han A, White B, Krause G, DeGracia D 2001 Brain ischemia and reperfusion activates the eukaryotic initiation factor 2α kinase, PERK. *J Neurochem* **77:** 1418–1421

Landau N, Littman D 1992 Packaging system for rapid production of murine leukemia virus vectors with variable tropism. *J Virol* **66:** 5110–5113

Liu CY, Schroder M, Kaufman RJ 2000 Ligand-independent dimerization activates the stress-response kinases IRE1 and PERK in the lumen of the endoplasmic reticulum. *J Biol Chem* **275:** 24881–24885

Lockhart DJ, Dong H, Byrne MC, Follettie MT, Gallo MV, Chee MS, Mittmann M, Wang C, Kobayashi M, Horton H, Brown EL 1996 Expression monitoring by hybridization to high-density oligonucleotide arrays. *Nat Biotechnol* **14:** 1675–1680

Maher P, Davis JB 1996 The role of monoamine metabolism in oxidative glutamate toxicity. *J Neurosci* **16:** 6394–6401

McCullough KD, Martindale JL, Klotz LO, Aw TY, Holbrook NJ 2001 Gadd153 sensitizes cells to endoplasmic reticulum stress by down-regulating Bcl2 and perturbing the cellular redox state. *Mol Cell Biol* **21:** 1249–1259

Miyamoto M, Murphy TH, Schnaar RL, Coyle JT 1989 Antioxidants protect against glutamate-induced cytotoxicity in a neuronal cell line. *J Pharmacol Exp Ther* **250:** 1132–1140

Morgenstern JP, Land H 1990 Advanced mammalian gene transfer: high titre retroviral vectors with multiple drug selection markers and a complementary helper-free packaging cell line. *Nucleic Acids Res* **18:** 3587–3596

Morimoto BH, Koshland Jr DE 1990 Induction and expression of long- and short-term neurosecretory potentiation in a neural cell line. *Neurone* **5:** 875–880

Murphy TH, Miyamoto M, Sastre A, Schnaar RL, Coyle JT 1989 Glutamate toxicity in a neuronal cell line involves inhibition of cystine transport leading to oxidative stress. *Neurone* **2:** 1547–1558

Novoa I, Zeng H, Harding H, Ron D 2001 Feedback inhibition of the unfolded protein response by GADD34-mediated dephosphorylation of eIF2α. *J Cell Biol* **153:** 1011–1022

Novoa I, Zhang Y, Zeng H, Jungreis R, Harding HP, Ron D 2003 Stress-induced gene expression requires programmed recovery from translational repression. *EMBO J* **22:** 1180–1187

Ron D, Harding H 2000 PERK and translational control by stress in the endoplasmic reticulum. In *Translational Control*, Hershey J, Mathews M, Sonenberg N (eds) pp 547–560. Cold Spring Harbor: CSHL Press

Scheuner D, Song B, McEwen E, Gillespie P, Saunders T, Bonner-Weir S, Kaufman RJ 2001 Translational control is required for the unfolded protein response and *in-vivo* glucose homeostasis. *Mol Cell* **7:** 1165–1176

Schubert D, Piasecki D 2001 Oxidative glutamate toxicity can be a component of the excitotoxicity cascade. *J Neurosci* **21:** 7455–7462

Spencer DM, Wandless TJ, Schreiber SL, Crabtree GR 1993 Controlling signal transduction with synthetic ligands. *Science* **262:** 1019–1024

Srivastava SP, Kumar KU, Kaufman RJ 1998 Phosphorylation of eukaryotic translation initiation factor 2 mediates apoptosis in response to activation of the double-stranded RNA-dependent protein kinase. *J Biol Chem* **273:** 2416–2423

Tan S, Sagara Y, Liu Y, Maher P, Schubert D 1998a The regulation of reactive oxygen species production during programmed cell death. *J Cell Biol* **141:** 1423–1432

Tan S, Somia N, Maher P, Schubert D 2001 Regulation of antioxidant metabolism by translation initiation factor 2alpha. *J Cell Biol* **152:** 997–1006

Tan S, Wood M, Maher P 1998b Oxidative stress induces a form of programmed cell death with characteristics of both apoptosis and necrosis in neuronal cells. *J Neurochem* **71:** 95–105

Zhang P, McGrath B, Li S, Frank A, Zambito F, Reinert J, Gannon M, Ma K, McNaughton K, Cavener DR 2002a The PERK eukaryotic initiation factor 2 alpha kinase is required for the development of the skeletal system, postnatal growth, and the function and viability of the pancreas. *Mol Cell Biol* **22:** 3864–3874

Zhang P, McGrath BC, Reinert J, Olsen DS, Lei L, Gill S, Wek SA, Vattem KM, Wek RC, Kimball SR, Jefferson LS, Cavener DR 2002b The GCN2 eIF2alpha kinase is required for adaptation to amino acid deprivation in mice. *Mol Cell Biol* **22:** 6681–6688

Zinszner H, Kuroda M, Wang X, Batchvarova N, Lightfoot RT, Remotti H, Stevens JL, Ron D 1998 CHOP is implicated in programmed cell death in response to impaired function of the endoplasmic reticulum. *Genes Dev* **12:** 982–995